

**FHS PUBLIC ACCESS**

Author manuscript

*J Biomed Mater Res B Appl Biomater.* Author manuscript; available in PMC 2017 July 18.

Published in final edited form as:

*J Biomed Mater Res B Appl Biomater.* 2015 February ; 103(2): 324–331. doi:10.1002/jbm.b.33205.**Grafting MAP peptide to dental polymer inhibits MMP-8 activity****Namrata Dixit<sup>1</sup>, Jenifer K. Settle<sup>1,2</sup>, Qiang Ye<sup>1</sup>, Cindy L. Berrie<sup>2</sup>, Paulette Spencer<sup>1,3</sup>, and Jennifer S. Laurence<sup>1,4</sup>**<sup>1</sup>Bioengineering Research Center, University of Kansas, Lawrence, Kansas 66045-7609<sup>2</sup>Department of Chemistry, University of Kansas, Lawrence, Kansas 66045<sup>3</sup>Department of Mechanical Engineering, University of Kansas, Lawrence, Kansas 66045<sup>4</sup>Department of Pharmaceutical Chemistry, University of Kansas, Lawrence, Kansas 66047**Abstract**

Matrix metalloproteinases (MMPs) are a class of zinc and calcium-dependent endopeptidases responsible for degrading extracellular matrix (ECM) components. Their activity is critical for both normal biological function and pathological processes (Dejonckheere et al., *Cytokine Growth Factor Rev* 2011;22:73–81). In dental restorations, the release and subsequent acid activation of MMPs contributes to premature failure. In particular, MMP-8 accelerates degradation by cleaving the collagen matrix within the dentin substrate in incompletely infiltrated aged bonded dentin (Buzalaf et al., *Adv Dent Res* 2012;24:72–76), hastening the need for replacement of restorations. Therefore, development of a dental adhesive that better resists MMP-8 activity is of significant interest. We hypothesize that modification of the polymer surface with an inhibitor would disable MMP-8 activity. Here, we identify the metal abstraction peptide (MAP) as an inhibitor of MMP-8 and demonstrate that tethering MAP to methacrylate polymers effectively inhibits catalysis. Our findings indicate complete inhibition of MMP-8 is achievable using a grafting approach. This strategy has potential to improve longevity of dental adhesives and other polymers and enable rational design of a new generation of biocompatible materials.

**Keywords**

MMP-8; dental adhesive; grafting; inhibitor; metal abstraction peptide; fluorescence assay

**INTRODUCTION**

Matrix metalloproteinase (MMP) activity remains a prime concern in the longevity of biocompatible polymers, including dental adhesives.<sup>1</sup> The prevention and treatment of tooth decay are major challenges in dentistry and annual expenditures associated with dental services surpass \$100 billion dollars in the US.<sup>2</sup> A substantial portion of this economic

---

**Correspondence to:** Jennifer S. Laurence ([laurencj@ku.edu](mailto:laurencj@ku.edu)) and P. Spencer ([pspencer@ku.edu](mailto:pspencer@ku.edu)).

Additional Supporting Information may be found in the online version of this article.

The authors declare the following competing financial interest: JSL is co-owner of Echogen Inc., which has licensed the patent-protected MAP Tag technology from the University of Kansas.

burden arises from the need for replacement of dental restorations. Dental materials are softer and more porous than the mineralized tooth and as such leach bioactive molecules from dentin that activate key enzymatic reactions, particularly MMPs.<sup>3</sup> These host-derived enzymes degrade the supporting tooth structure to which the adhesive is attached and facilitate destruction of the bonded interface.<sup>4</sup>

The MMP family is large and its members act on diverse substrates specific to individual tissues. Mature human odontoblasts secrete the gelatinases MMP-2 and -9, collagenases MMP-8 and -13, and enamelysin MMP-20.<sup>3</sup> The organic fraction of dentin is composed predominantly of type I collagen, and cleavage of this matrix is primarily accomplished by MMP-8. As such, inhibition of MMP-8<sup>5</sup> is critical to developing next-generation dental adhesives.

In normal biological processes the activity of MMPs is regulated by inhibitory proteins such as  $\alpha$ 2-macroglobulin (a plasma protein that acts as general protease inhibitor) and specific tissue inhibitors of MMPs (TIMP-1, -2, -3, and -4). Unfortunately, due to the expense and limited stability in the oral environment, large proteins such as these are not viable options for use in a biomaterial. Over the last 20 years a tremendous amount of effort has been made to develop small molecule<sup>6,7</sup> and peptide inhibitors capable of controlling these enzymes and the disease conditions that result from aberrant activity.<sup>8-10</sup> Despite substantial efforts, successful introduction of a MMP-8 inhibitor into a dental adhesive has not yet been reported. Design of MMP-8 inhibitors has been challenging due to the large size of this enzyme's binding pocket, particularly the S1 specific loop.<sup>11</sup> This flexible loop of MMP-8 does not favor tight binding, making potent inhibition difficult to accomplish using small molecules.<sup>11</sup> As such, peptides may offer the best option for inhibiting MMP-8.

Peptide-polymer conjugates are a promising new class of versatile materials that leverage the advantage of stable polymer combined with hierarchical structure and chemical functionality of peptides.<sup>12</sup> In the last decade, much work has been done in modifying polymer surfaces for various signaling and biomolecule immobilization studies,<sup>13-18</sup> but these approaches have yet to be applied to dental restorations. The approach presented (Figure 1) entails grafting a peptide-based inhibitor onto an amine-containing polymerized resin to inhibit MMP-8 activity at the exposed surface. Grafting avoids pitfalls associated with use of soluble inhibitors. By restricting inhibition solely to the location of interest, MMPs in the immediate vicinity are selectively affected. In addition, unlike leachable strategies in which it is difficult to incorporate sufficient amounts of inhibitor to persist for long durations of time and the material becomes more porous as the inhibitor diffuses out, grafting does not necessarily disrupt the structure of the adhesive polymer or lose activity as quickly over time. The first crucial step in this pursuit was to identify a peptide sequence that inhibits MMP-8. The metal abstraction peptide (MAP) technology reported by the Laurence lab,<sup>19</sup> provides a new approach with great potential for accomplishing MMP inhibition at polymer surfaces. MAP is a tripeptide with a unique chemistry capable of robbing transition metal ions, such as  $Zn^{2+}$ , from chelators.<sup>19</sup> Because the functional unit of MAP is only three amino acids long, the inhibitory peptide can be engineered to suit the length and geometry of a target protein. Here, the MAP module was incorporated into a

longer peptide (tether-MAP) and grafted to amine-containing polymers, and the ability of the functionalized polymer to deactivate MMP-8 was investigated.

## MATERIALS AND METHODS

2,2-bis[4-(2-hydroxy-3-methacryloxypropoxy)phenyl]-propane (BisGMA, Polysciences, Warrington, PA) and 2-hydroxyethyl methacrylate (HEMA, Acros Organics, NJ) were used as received without further purification as monomers in dentin adhesives. 2-Aminoethyl methacrylate hydrochloride (AEMA) was used as a co-monomer as obtained from Sigma Aldrich (St. Louis, MO). Camphoroquinone (CQ) and ethyl-4-(dimethylamino)benzoate (EDMAB) were obtained from Sigma-Aldrich (St. Louis, MO). All other chemicals were reagent grade and used without further purification. MMP-8 colorimetric and fluorimetric RED kits were bought from Enzo life sciences and used as instructed. Peptides Asn-Cys-Cys (MAP), Ser-Trp-Leu-Ala-Tyr-Pro-Gly-Ala-Val-Ser-Tyr-Arg-Gly-Asn-Cys-Cys (tether-MAP), and Disuccinimidyl suberate (DSS) linker were gifts from Echogen Inc.

### Preparation of polymer resins

The control adhesive consisted of HEMA and BisGMA with a mass ratio of 60/40% w/w (HEMA/BisGMA). The photoinitiators used in this study were 0.5% w/w each camphorquinone (CQ), ethyl 4-(dimethylamino)benzoate (EDMAB) and diphenyliodonium hexafluorophosphate (DPIHP). All these materials were used as received. The experimental adhesives were formulated with 5, 10, 15, and 20% w/w AEMA monomer to facilitate grafting on the surface. Mixtures of monomers/photoinitiators were prepared in a brown glass vial in the absence of visible light. The solutions containing the monomers/photoinitiators were mixed overnight at room temperature to promote complete dissolution and formation of a homogeneous solution prior to light-induced polymerization.

### Degree of conversion

The DC and polymerization behavior was determined by FTIR as described previously by our group.<sup>20</sup> Real-time *in situ* monitoring of the photo-polymerization of the different adhesive solutions was performed using an infrared spectrometer (Spectrum 400 Fourier transform infrared spectrophotometer, Perkin-Elmer, Waltham, MA) at a resolution of 4  $\text{cm}^{-1}$ . One drop of adhesive solution was placed on the diamond crystal top plate of an attenuated total reflectance (ATR) accessory (PIKE Technologies Gladi-ATR, Madison, WI) and covered with a cover slip to prevent oxygen inhibition of polymerization. A 40-s exposure to the commercial visible-light-polymerization unit (SpectrumVR 800, Dentsply, Milford, DE) at an intensity of 550  $\text{mW cm}^{-2}$  was initiated after 50 spectra had been recorded. Real-time IR spectra were continuously recorded for 900 s after light activation began. A time-based spectrum collector (Spectrum Time-Base, Perkin-Elmer) was used for continuous and automatic collection of spectra during polymerization. Three replicates were obtained for each adhesive formulation. The change of the band ratio profile [ $1637 \text{ cm}^{-1}$  (C=C)/ $1608 \text{ cm}^{-1}$  (phenyl)] was monitored and degree of conversion (DC) was calculated using the following equation, where A = absorbance, based on the decrease in the absorption intensity band ratio before and after light curing,<sup>20</sup> as in Eq. (1) below.

$$DC = \left[ 1 - \frac{A_{\text{polymer}} 1637 \text{ cm}^{-1} / A_{\text{polymer}} 1608 \text{ cm}^{-1}}{A_{\text{monomer}} 1637 \text{ cm}^{-1} / A_{\text{monomer}} 1608 \text{ cm}^{-1}} \right] \times 100\% \quad (1)$$

### Resin coating of 96-well plate

To make the polymer coating on a 96-well plate, 40  $\mu\text{L}$  of each resin formulation was aliquoted in different wells and cured with a 40-s exposure to the commercial visible-light-polymerization unit (Spectrum VR 800, Dentsply, Milford, DE) at an intensity of 550  $\text{mW cm}^{-2}$ . The plate was left under dark for post polymerization for 48 h.

Polymerization and curing in the 96-well plates were performed using atmospheric conditions and oxygen-depleted conditions in which the plate was placed in a sealed enclosure and purged with nitrogen for 5 min. Samples produced with and without oxygen depletion behaved comparably.

### Methyl orange assay

Methyl orange assays were conducted with a few modifications from literature procedures.<sup>21</sup> A 0.2% methyl orange (Fisher Scientific) stock solution was prepared using deionized water. This solution was diluted to 0.05% with 0.1  $M \text{NaH}_2\text{PO}_4$  solution (solid from Fisher Scientific) to prepare an acidic methyl orange solution (final buffer concentration was 0.075  $M \text{NaH}_2\text{PO}_4$  solution).

Polymers were presoaked in water for 2–7 days to remove any leachables. Polymers were removed from water, rinsed under a stream of deionized water for approximately 10–30 s, and excess water was removed by blotting samples on a Kimwipe. Polymers were then incubated in acidic methyl orange solution for ~1 h. Polymers were removed from solution, rinsed under a stream of deionized water for approximately 10–30 s, and excess water was removed by blotting samples on a Kimwipe. A 0.1  $M \text{Na}_2\text{CO}_3$  (Fisher Scientific) solution was prepared (base solution). Polymers were incubated in 5 mL of base solution for ~6.5 h. The absorbance of the resultant base solution (with methyl orange extracted from the polymer samples) was measured using a UV-Vis spectrophotometer (Thermo Scientific Evolution300 UV-VIS) from 400–800 nm. Methyl orange has a maximum absorbance at 465 nm. The concentration was determined by using a standard calibration curve with the dye solution at different concentrations. This curve was linear over the concentration range investigated here. The concentration can be used to determine the amount of dye in the solution, which can be used to estimate the number of adsorbed methyl orange molecules per mass of polymer.

### Peptide grafting on polymer surfaces

DSS linker chemistry was used to graft the inhibitor peptide on to the polymer surfaces via amine containing residues. The reaction volume was limited to 50  $\mu\text{L}$  so that the reactants could remain mostly localized on the polymer surface and tried different concentration ratios of DSS and tether-MAP. 47  $\mu\text{L}$  of HEPES buffer pH 7.4, 2  $\mu\text{L}$  of 1  $M$  peptide and 1  $\mu\text{L}$  of 50  $mM$  DSS linker were used per well. The plate was incubated at room temp for 1 h and

then the reaction was quenched by adding 50  $\mu\text{L}$  of 20 mM Tris buffer for 15 min. Wells were then washed ten times with 400  $\mu\text{L}$  dd  $\text{H}_2\text{O}$  prior to data acquisition. A positive control was performed with 4'-(aminomethyl) fluorescein, hydrochloride (Invitrogen) under the same conditions over all polymer surfaces.

### MMP-8 activity RED fluorometric assay

MMP-8 Fluorometric Drug Discovery Kit, RED was used to study MMP inhibition on polymer surfaces. This kit also contains the same NNGH standard inhibitor as in colorimetric kit. The components were diluted in assay buffer that had been pre-warmed to the reaction temperature (37°C). The fluorescent microplate reader was calibrated using Ex/Em = 545/576 nm, with cutoff set at 570 nm.

The assays are performed in a convenient 96-well micro-plate format. NNGH was diluted 1/200 in assay buffer to required total volume and warmed to reaction temperature 37°C. Substrate peptide was diluted 1/50 in assay buffer to required total volume. MMP-8 enzyme was diluted 1/100 in assay buffer to required total volume and warmed to reaction temperature 37°C. Assay buffer was pipetted into each desired well as follows: Blank (no MMP-8) = 90  $\mu\text{L}$  assay Buffer, control (no inhibitor) = 70  $\mu\text{L}$  assay Buffer and Inhibitor NNGH and test inhibitors = 50  $\mu\text{L}$  assay Buffer. 20  $\mu\text{L}$  of MMP-8 was added in all wells except the blank followed by 20  $\mu\text{L}$  of inhibitor NNGH (final inhibitor concentration=1.3  $\mu\text{M}$ ) in NNGH designated wells and different concentrations of test inhibitor peptides (final concentrations of 0.01, 0.1, 1.0  $\mu\text{M}$ ) in respective wells. The plate was incubated for 90 min at reaction temperature 37°C to allow inhibitor/enzyme interaction and then 10  $\mu\text{L}$  of substrate peptide (diluted and equilibrated to reaction temperature) was added (final substrate concentration = 100  $\mu\text{M}$ ) to start the reaction. The plate was read continuously in the fluorescent microplate reader, using Ex/Em = 545/576 nm, with cutoff set at 570 nm at set reaction temperature 37°C.

## RESULTS

### Degree of conversion of polymer resins

Standard adhesive formulation of HEMA and Bis-GMA was doped with different wt % of AEMA monomer to facilitate peptide grafting onto the polymer surface. To determine the effect of altering the standard formulation to incorporate AEMA, the degree of conversion (DC) for each resin formulation was examined. Because AEMA is poorly soluble in BisGMA, the control resin has a higher proportion of HEMA than is standard in order to accommodate up to 20% AEMA. Real-time photo-polymerization kinetic behavior of the control and experimental adhesives is shown in Figure 2. It is evident that addition of AEMA has an effect on DC. With increasing AEMA content, DC increased from 61% for the control resin to 70–80% for the experimental resins. At each level of AEMA content, the polymerization rates of the experimental adhesives were significantly higher than those of the control. The standard adhesive formulation, however, has a DC of ~70%, which is well matched by the 15–20% AEMA-containing samples.

### Determination of solvent-accessible amine content

Methyl orange (MO) electrostatically binds to the available amines within the polymer and is extracted using basic solution. UV-Vis analysis of the series of extracts containing methyl orange have increased absorbance at 465 nm, and the intensities reflect the increasing amount of solvent accessible amines within the polymer, corresponding to the expected percent increase in incorporated amine within the polymer. Figure 3(a) depicts that correlation, indicating the increase in amine content resulted in a proportional increase in methyl orange adsorption and extraction from the polymers. This confirms that a higher percentage of amine within the polymer formulation results in additional solution-accessible amine sites incorporated within the polymer.

### Peptide grafting onto polymer surfaces

The adhesive resin formulations were polymerized in 96-well plates in order to carry out grafting and inhibition studies. An amine moiety is present on both the peptide and polymer, and this moiety is used to accomplish linking the two species via DSS. Because DSS is a homobifunctional linker, self-coupling between soluble peptides occurs readily in solution. A series of experimental conditions were examined to optimize the grafting reaction. As a positive control, the matrix was repeated using FITC instead of tether-MAP. Grafting of tether-MAP, monitored by intrinsic tryptophan fluorescence ( $E_{ex}/E_{em} = 280/360$ ), follows an almost linear trend of RFU with AEMA content in polymer resin [Figure 3(b)]. The positive control with FITC, measured at  $E_{ex}/E_{em} = 492/516$ , follows the same trend [Figure 3(b)]. The findings indicate 10 mM DSS and 0.1 mM peptide/dye is the optimum condition for efficient grafting. These results parallel the trend observed for solvent accessible amine content, determined above using the MO assay.

### Analysis of residual solvent-accessible amines following grafting

To quantify the unreacted amine content in the polymer following completion of the coupling reaction, the methyl orange assay was applied to dye-conjugated polymers. As a control, MO was applied to the control formulation before and after carrying out the grafting reaction. As expected, no discernible difference in MO adsorption is observed for the control formulation because grafting cannot occur. A decrease in absorbance at 465 nm is observed for the 5%, 10%, 15%, and 20% amine-containing polymers after DSS-dye coupling when compared with unmodified samples of the same composition. In all cases, the absorbance at 465 nm decreased by ~80% after grafting [Figure 3(a)]. The 20% residual amine content may be due to restricted accessibility to the surface by the larger linker-peptide compared with MO, which is consistent with the data showing that increasing the concentration of the reaction components does not lead to greater grafting efficiency.

### MMP-8 inhibitor analysis

To examine the ability of the MAP peptide module (asparagine–cysteine–cysteine; NCC) to inhibit MMP-8 a standard fluorimetric assay first was carried out in solution. The MAP peptides were tested and compared with positive and negative control reactions. Figure 4(a) shows that 0.1  $\mu$ M of NCC achieves nearly complete inhibition of MMP-8. 1.3  $\mu$ M of the standard inhibitor NNGH is required to achieve a similar result, whereas 0.1  $\mu$ M NNGH

achieves ~50% inhibition in similar conditions, indicating that perhaps MAP tag is a better inhibitor than NNGH.

To ensure accessibility of the inhibitory peptide module and permit interaction with MMP-8 once tethered to the polymer, MAP was incorporated into a longer polypeptide to provide a spacer between the inhibitory MAP module and the polymer surface. Based on examination of the MMP-8 structure and literature reports on structure activity relationships of MMP-8 inhibitors, a 13 amino acid spacer was chosen, which includes a tryptophan for quantification. A 16 amino acid long peptide called tether-MAP was generated with MAP at the C-terminus (Figure 5). The tether-MAP peptide was tested for its ability to inhibit MMP-8 activity in solution. It was found to require ~10-fold higher concentration than the MAP tripeptide alone, but tether-MAP completely abrogated turn over at comparable or slightly lower concentration than NNGH [Figure 4(b)].

To verify the peptide remains functional as an inhibitor after tethering to the polymer surface, the MMP-8 assay was carried out on the series of peptide-grafted polymer surfaces, including control resin, 5%, 10%, and 20% AEMA-doped resin. Each resin was first modified with tether-MAP peptide and then assayed as in solution and compared with control and NNGH reactions. In addition, the control and standard inhibitor reactions were run on the series of unconjugated, bare polymer resins to account for background and establish any differences caused by changes in polymer composition. All resins behaved comparably, indicating the polymer does not affect the assay and that the observed inhibition results from the grafted peptide. Figure 6 shows the efficiency of inhibition increased with increasing amount of grafted peptide, corresponding to the percent amine in the formulation. The 20% AEMA containing resin grafted with tether-MAP showed the best result, in which complete inhibition of MMP-8 was achieved.

## DISCUSSION

MMP inhibition remains a prime concern in development of new dental adhesives.<sup>22,23</sup> The set of investigations reported to date have established MMP-8 is more difficult to inhibit than other MMPs present in dentin, likely due to the large, flexible S1 loop in the binding pocket of MMP-8.<sup>11</sup> As such, peptides may better fill the pocket of MMP-8 compared with small molecules and may provide a better starting place for understanding how to design selective inhibitors to this key enzyme. The MAP chemistry applies to transition metals, including zinc, and as such, the MAP technology provides a new tool to address this critical issue. Here, tether-MAP was engineered to suit the length and geometry of the target protein and demonstrates effective inhibition of MMP-8 is retained when grafted to the polymer surface, suggesting that MAP binds the zinc ion present in MMP-8 and disables enzymatic function.

The quality of the adhesive bond to the dentin substrate is closely related to infiltration and photo-polymerization of adhesive resins.<sup>24,25</sup> DC value is one critical parameter that reflects the quality of the adhesive bond and the interfacial hybrid layer.<sup>26-28</sup> Better infiltration into the demineralized collagen substrate results in greater contact area between the tooth and restoration, which supports tight bonding. Infiltration in part is limited by viscosity of the resin formulation. Here, the standard formulation was modified to support miscibility of the

amine-containing monomer, which was used to functionalize the polymer for grafting. The observed increase in DC of AEMA-containing resins may be attributed to decreased viscosity, resulting from the lower BisGMA content. Lower viscosity would have the added benefit that it may improve infiltration into the dentin prior to polymerization, facilitating better integration with the collagenous substrate.

Polymerized samples containing AEMA were shown to display solvent-accessible amines both before and after grafting. The amount of amine detected was proportional to the amount of AEMA included in the resin, and 80% efficiency of attachment was observed for all samples modified using DSS chemistry, regardless of polymer composition and the species attached. In both the fluorescence and methyl orange assays the surface-accessible amine concentration dependence appears to be nonlinear with respect to the AEMA concentration in the resin. This suggests the solvent-accessible amine content is affected by chemical and/or structural changes in the polymer. The effect may emanate from variation in the formulation's overall hydrophobicity, which may perturb the pKa and/or reactivity of the amine differently in the context of resin mixtures having differing properties.<sup>29</sup> Relative proportions of individual components may also affect surface accessibility of the amine groups and crosslinking density by modulating viscosity and/or miscibility. Our results here demonstrate increasing the proportion of amine-containing monomer in the formulation disproportionately elevates the solvent accessible amine content, facilitating grafting to these moieties. Nonetheless, the ratio of reacted to residual amines remains constant at approximately 4:1.

The persistence of 20% residual unreacted amine following grafting suggests incorporation of amine moieties may provide multifunctionality, in which the grafted peptide specifically staves off the destructive action of MMPs while unreacted amines act as a proton sponge to moderate the effects of chemical degradation caused by the acidic oral environment.<sup>29-31</sup> In addition to MMP activity, a second key factor that contributes to premature failure of composite restorations is recurrent caries at the margins of these restorations.<sup>26,32</sup> This phenomenon is linked to attachment of the cariogenic bacterium *Streptococcus mutans*.<sup>33</sup> Adhesion of *S. mutans* to the tooth surface supports subsequent growth and recruitment of additional bacteria. Microbial metabolism generates lactic acid, which demineralizes the tooth and further activates MMPs. Efforts to address bacterial adhesion and MMP activity have primarily relied on incorporation of a quaternary ammonium salt.<sup>7</sup> Incorporation of quaternary ammonium methacrylate comonomer also has been examined but this approach required higher concentration.<sup>34</sup> These moieties are nonspecific in their mechanism of action and affect a wide variety of MMPs. The advantage of the comonomer approach over the salt is that it is not readily leachable and remains in place. In this study, primary amine moieties are used to tether an inhibitory peptide to the methacrylate polymer to achieve specific inhibition. Separately, our group reported amine-containing monomers may act as a proton sponge and help neutralize lactic acid.<sup>35</sup> Combining these approaches creates the opportunity to combat synergistically both acid and enzyme-based degradation.

This study presents a first step toward the goal of increased longevity of dental restorations by inhibiting collagen degradation. To advance this approach toward clinical application, further *in situ* and *in vivo* studies must be performed. More complete characterization of the



interaction between MAP and MMP-8 is being pursued with the aim of improving potency against and selectivity for inhibition of MMP-8 to enable further optimization of the grafted inhibitor. To advance this approach into the clinic, the amine-containing and grafted adhesive formulations next must be applied to collagenous dentin substrates and the rate of collagen degradation determined to be reduced significantly. In addition, the mechanical properties of the modified adhesive formulations and the long-term integrity of the restoration, including both the adhesive and grafted peptide, also will need to be demonstrated *in vivo*. Having confirmed the initial hypothesis that surface modification with tether-MAP inhibits MMP-8 has laid the foundation for these subsequent studies to be pursued.

## CONCLUSIONS

The MAP peptide was shown to effectively inhibit MMP-8 and its inhibitory function is retained when tethered to the polymer surface via a spacer. The standard dental adhesive resin formulation was modified to incorporate functionality for peptide grafting, and incorporation of AEMA produced polymers with the desired degree of conversion. We identified an efficient way to graft peptide to the polymer and achieved complete inhibition of MMP-8 at the polymer surface. Optimization of the composition of the dental adhesive formulation to maximize performance characteristics clearly involves multiple parameters. Here, we highlight that amine moieties may be used to functionalize the polymer surface and protect against degradation by MMP enzymes.

## Acknowledgments

The authors thank Drs. Mary Krause and Qingxin Mu for helpful discussion and technical assistance. The authors thank Echogen for donation of tether-MAP.

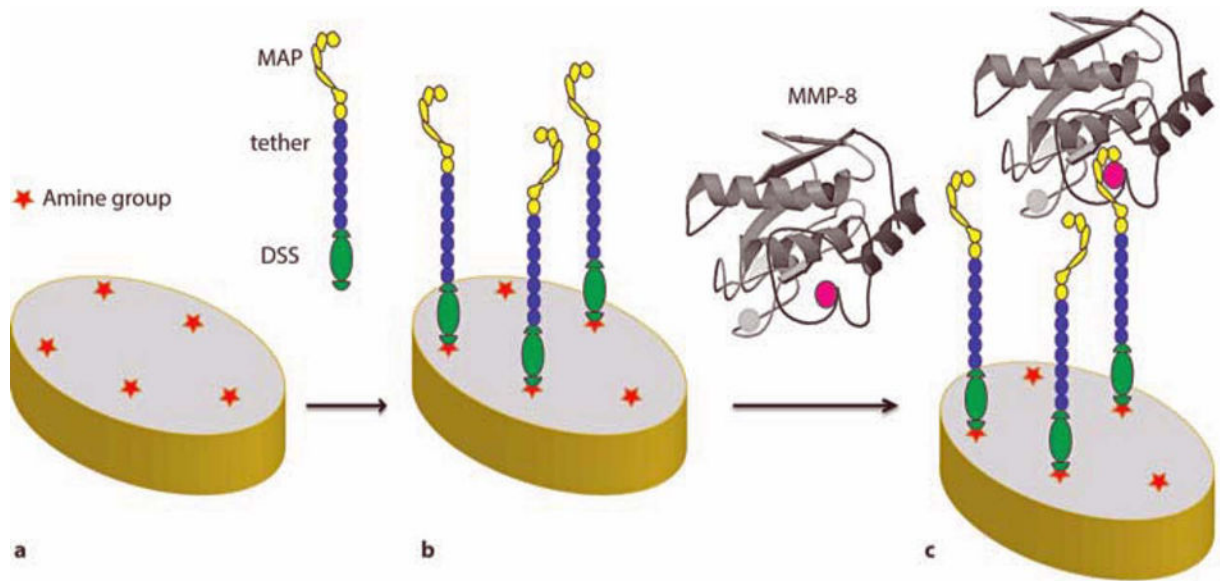
Contract grant sponsor: NIH/NIDCR; contract grant numbers: R01DE14392, R01DE22054

## References

1. De Munck J, Van den Steen PE, Mine A, Van Landuyt KL, Poitevin A, Opdenakker G, Van Meerbeek B. Inhibition of enzymatic degradation of adhesive-dentin interfaces. *J Dent Res*. 2009; 88:1101–1106. [PubMed: 19861692]
2. Spencer P, Ye Q, Park J, Misra A, Bohaty BS, Singh V, Parthasarathy R, Sene F, Gonçalves S, Laurence J. Durable bonds at the adhesive/dentin interface: An impossible mission or simply a moving target? *Braz Dent Sci*. 2012; 15:4–18. [PubMed: 2485586]
3. Milia E, Cumbo E, Cardoso RJA, Gallina G. Current dental adhesives systems. A narrative review. *Current Pharmaceutical Des*. 2012; 18:5542–5552.
4. Tjaderhane L, Nascimento FD, Breschi L, Mazzoni A, Tersariol ILS, Geraldeli S, Tezvergil-Mutluay A, Carrilho MR, Carvalho RM, Tay FR, Pashley DH. Optimizing dentin bond durability: Control of collagen degradation by matrix metalloproteinases and cysteine cathepsins. *Dental Mater*. 2013; 29:116–135.
5. Sulkala M, Tervahartiala T, Sorsa T, Larmas M, Salo T, Tjaderhane L. Matrix metalloproteinase-8 (MMP-8) is the major collagenase in human dentin. *Arch Oral Biol*. 2007; 52:121–127. [PubMed: 17045563]
6. Hu J, Van den Steen PE, Sang Q-XA, Opdenakker G. Matrix metalloproteinase inhibitors as therapy for inflammatory and vascular diseases. *Nat Rev Drug Discov*. 2007; 6:480–498. [PubMed: 17541420]

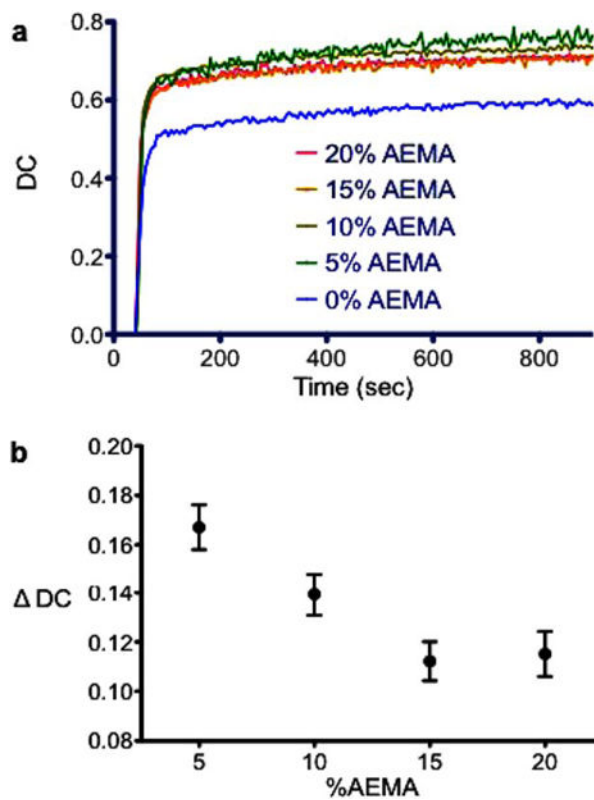
7. Tezvergil-Mutluay A, Mutluay MM, Gu LS, Zhang K, Agee KA, Carvalho RM, Manso A, Carrilho M, Tay FR, Breschi L, et al. The anti-MMP activity of benzalkonium chloride. *J Dent.* 2011; 39:57–64. [PubMed: 20951183]
8. Jacobsen JA, Fullagar JL, Miller MT, Cohen SM. Identifying chelators for metalloprotein inhibitors using a fragment-based approach. *J Med Chem.* 2011; 54:591–602. [PubMed: 21189019]
9. Krizkova S, Zitka O, Masarik M, Adam V, Stiborova M, Eckschlager T, Chavis GJ, Kizek R. Assays for determination of matrix metalloproteinases and their activity. *Trac-Trends Anal Chem.* 2011; 30:1819–1832.
10. Ndinguri MW, Bhowmick M, Tokmina-Roszyk D, Robichaud TK, Fields GB. Peptide-based selective inhibitors of matrix metalloproteinase-mediated activities. *Molecules.* 2012; 17:14230–14248. [PubMed: 23201642]
11. Dorman G, Cseh S, Hajdu I, Barna L, Konya D, Kupai K, Kovacs L, Ferdinandy P. Matrix metalloproteinase inhibitors: A critical appraisal of design principles and proposed therapeutic utility. *Drugs.* 2010; 70:949–964. [PubMed: 20481653]
12. Shu JY, Panganiban B, Xu T. Peptide-polymer conjugates: From fundamental science to application. *Annual Rev Phys Chem.* 2013; 64:631–657. [PubMed: 23331303]
13. Sikes HD, Hansen RR, Johnson LM, Jenison R, Birks JW, Rowlen KL, Bowman CN. Using polymeric materials to generate an amplified response to molecular recognition events. *Nat Mater.* 2007; 7:52–56. [PubMed: 17965717]
14. Place ES, Evans ND, Stevens MM. Complexity in biomaterials for tissue engineering. *Nat Mater.* 2009; 8:457–470. [PubMed: 19458646]
15. Dominique AR, Harry B, Conlin PON, Jeffrey AH. Biofunctional polymer nanoparticles for intra-articular targeting and retention in cartilage. *Nat Mater.* 2008; 7:248–254. [PubMed: 18246072]
16. Grafahrend D, Heffels KH, Beer MV, Gasteier P, Moller M, Boehm G, Dalton PD, Groll J. Degradable polyester scaffolds with controlled surface chemistry combining minimal protein adsorption with specific bioactivation. *Nat Mater.* 2011; 10:67–73. [PubMed: 21151163]
17. Jiang H, Xu F-J. Biomolecule-functionalized polymer brushes. *Chem Soc Rev.* 2013; 42:3394–3426. [PubMed: 23348574]
18. Kuroki H, Tokarev I, Minko S. Responsive surfaces for life science applications. *Annual Rev Mater Res.* 2012; 42:343–372.
19. Krause ME, Glass AM, Jackson TA, Laurence JS. MAPping the chiral inversion and structural transformation of a metaltripeptide complex having ni-superoxide dismutase activity. *Inorganic Chem.* 2011; 50:2479–2487.
20. Ye Q, Park J, Topp E, Spencer P. Effect of photoinitiators on the in vitro performance of a dentin adhesive exposed to simulated oral environment. *Dent Mater.* 2009; 25:452–458. [PubMed: 19027937]
21. Hartwig A, Mulder M, Smolders CA. Surface amination of poly(a-crylonitrile). *Adv Colloid Interface Sci.* 1994; 52:65–78.
22. Almahdy A, Koller G, Sauro S, Bartsch JW, Sherriff M, Watson TF, Banerjee A. Effects of MMP inhibitors incorporated within dental adhesives. *J Dent Res.* 2012; 91:605–611. [PubMed: 22518030]
23. Verma R, Singh UP, Tyagi SP, Nagpal R, Manuja N. Long-term bonding effectiveness of simplified etch-and-rinse adhesives to dentin after different surface pre-treatments. *J Conservative Dentistry JCD.* 2013; 16:367. [PubMed: 23956543]
24. Ye Q, Wang Y, Williams K, Spencer P. Characterization of photo-polymerization of dentin adhesives as a function of light source and irradiance. *J Biomed Mater Res B: Appl Biomater.* 2007; 80:440–446. [PubMed: 16850459]
25. Ye Q, Spencer P, Wang Y, Misra A. Relationship of solvent to the photopolymerization process, properties, and structure in model dentin adhesives. *J Biomed Mater Res A.* 2007; 80:342–350. [PubMed: 17001655]
26. Spencer P, Ye Q, Park J, Topp EM, Misra A, Marangos O, Wang Y, Bohaty BS, Singh V, Sene F. Adhesive/dentin interface: The weak link in the composite restoration. *Annals Biomed Eng.* 2010; 38:1989–2003.

27. Park J, Eslick J, Ye Q, Misra A, Spencer P. The influence of chemical structure on the properties in methacrylate-based dentin adhesives. *Dental Mater.* 2011; 27:1086–1093.
28. Park JG, Ye Q, Topp EM, Spencer P. Enzyme-catalyzed hydrolysis of dentin adhesives containing a new urethane-based trimethacrylate monomer. *J Biomed Mater Res Part B: Appl Biomater.* 2009; 91:562–571. [PubMed: 19582843]
29. Laurence JS, Nelson BN, Ye Q, Park J, Spencer P. Characterization of acid-neutralizing basic monomers in co-solvent systems by NMR. *Int J Polymeric Mater Polymeric Biomater. Int J Polymer Mater.* 2014; 63:361–367.
30. Park J, Ye Q, Spencer P, Laurence JS. Determination of neutralization capacity and stability of a basic methacrylate monomer using NMR. *Int J Polym Mater Polym Biomater.* 2012; 61:144–153. [PubMed: 22544985]
31. Li F, Chai ZG, Sun MN, Wang F, Ma S, Zhang L, Fang M, Chen JH. Anti-biofilm effect of dental adhesive with cationic monomer. *J Dent Res.* 2009; 88:372–376. [PubMed: 19407160]
32. Imbeni V, Kruzic JJ, Marshall GW, Marshall SJ, Ritchie RO. The dentin–enamel junction and the fracture of human teeth. *Nat Mater.* 2005; 4:229–232. [PubMed: 15711554]
33. Paul EK, Robert JP, Saravanan P, Nicholas SJ. Oral multispecies biofilm development and the key role of cell–cell distance. *Nat Rev Microbiol.* 2010; 8:471–480. [PubMed: 20514044]
34. Tezvergil-Mutluay A, Agee KA, Uchiyama T, Imazato S, Mutluay MM, Cadenaro M, Breschi L, Nishitani Y, Tay FR, Pashley DH. The inhibitory effects of quaternary ammonium methacrylates on soluble and matrix-bound MMPs. *J Dent Res.* 2011; 90:535–540. [PubMed: 21212315]
35. Park J, Ye Q, Spencer P, Laurence JS. Determination of neutralization capacity and stability of a basic methacrylate monomer using NMR. *Int J Polym Mater Polym Biomater.* 2012; 61:144–153.
36. Dejonckheere E, Vandenbroucke RE, Libert C. Matrix metalloproteinase8 has a central role in inflammatory disorders and cancer progression. *Cytokine Growth Factor Revi.* 2011; 22:73–81.
37. Buzalaf MA, Kato MT, Hannas AR. The role of matrix metalloproteinases in dental erosion. *Adv Dent Res.* 2012; 24:72–76. [PubMed: 22899684]

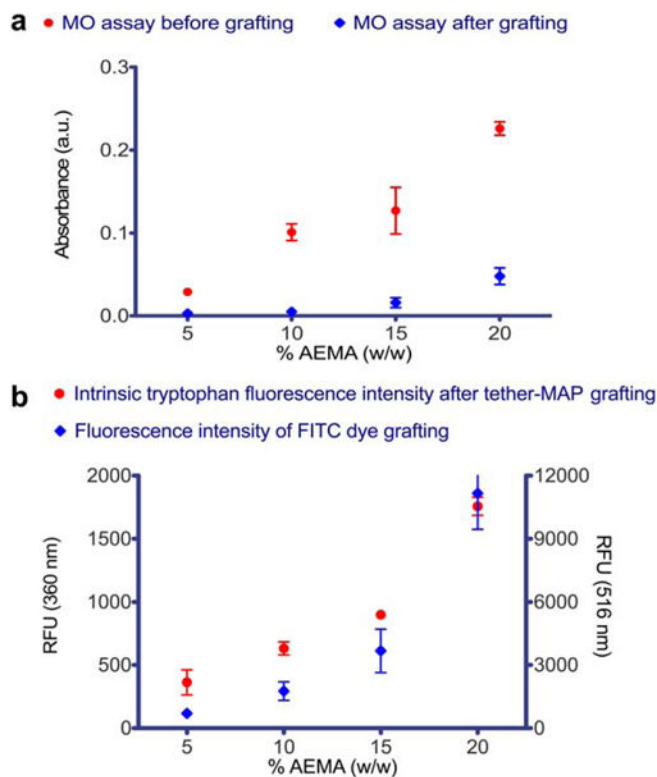


**FIGURE 1.**

Proposed construction of grafted polymer surface to inhibit MMP-8. (a) Amine-terminated polymer surfaces, (b) grafting of tether-MAP peptide to amines via DSS linker chemistry, (c) MMP-8 inhibition at polymer surface by MAP. MMP-8 structure code 2oy4 was downloaded from PDB. [Color figure can be viewed in the online issue, which is available at [wileyonlinelibrary.com](http://wileyonlinelibrary.com).]

**FIGURE 2.**

Degree of conversion (DC) of control and experimental resin formulations.  $DC = DC(\%AEMA) - DC(\text{control})$  at  $t = 900$  s as determined by FTIR using Eq. (1). The plots show DC of 5% AEMA monomer is highest among AEMA-doped polymers, whereas DC for 15% and 20% are virtually equivalent. The data are plotted relative to the control formulation, showing that all AEMA-containing formulations have significantly higher DC than the control. [Color figure can be viewed in the online issue, which is available at [wileyonlinelibrary.com](http://wileyonlinelibrary.com).]

**FIGURE 3.**

Effective coupling to polymer-incorporated amines is accomplished. Accessibility of amine functionality and grafting of peptide onto amine-doped polymer surfaces is shown. The Y-axis in panel a reflects methyl orange absorbance at 465 nm for the control (0%), 5%, 10%, 15%, and 20% amine-containing polymer samples before and after DSS coupling. The Y-axes in panel b show fluorescence intensity of grafted polymers in RFU. The left axis corresponds to the intrinsic fluorescence intensity ( $E_{ex}/E_{em} = 280/360$ ) of the single tryptophan residue in tether-MAP (red), and the right y-axis corresponds to the fluorescence intensity of grafted FITC ( $E_{ex}/E_{em} = 492/516$ ) (blue). [Color figure can be viewed in the online issue, which is available at [wileyonlinelibrary.com](http://wileyonlinelibrary.com).]

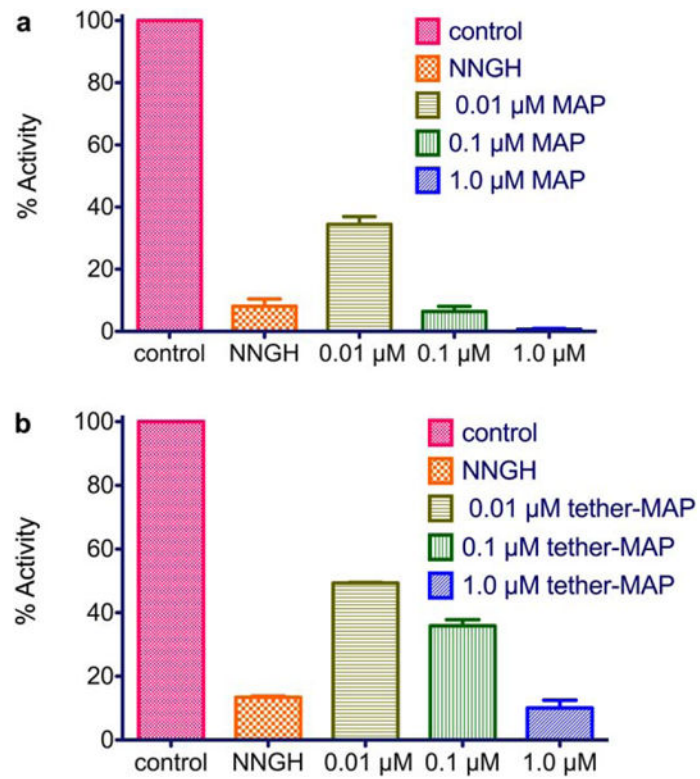


**FIGURE 4.**

MAP peptides inhibit MMP-8 activity in solution. A bar graph shows the % activity remaining at 30-min endpoint comparison from the MMP-8 fluorometric RED assay with increasing concentrations of MAP and tether-MAP. The standard inhibitor NNGH was used as a control. [Color figure can be viewed in the online issue, which is available at [wileyonlinelibrary.com](http://wileyonlinelibrary.com).]

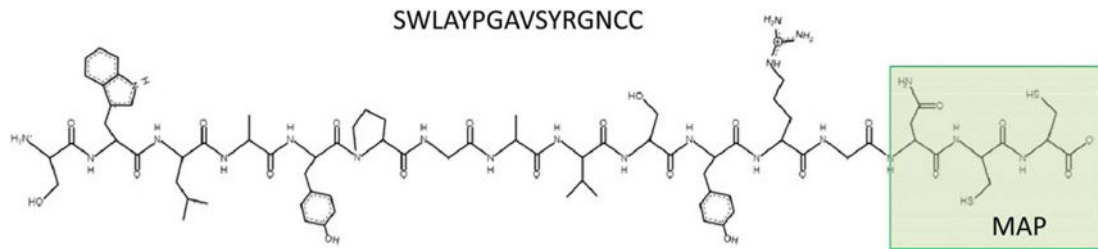


**FIGURE 5.**

Sequence and structure of tether-MAP peptide. Tether-MAP is 16 amino acids in length.

There is a 13 amino acid spacer, which contains a tryptophan (W) residue for quantitative

analysis. The MAP module positioned at the C-terminus is comprised of NCC (asparagine–

cysteine–cysteine). [Color figure can be viewed in the online issue, which is available at

[wileyonlinelibrary.com](http://wileyonlinelibrary.com).]



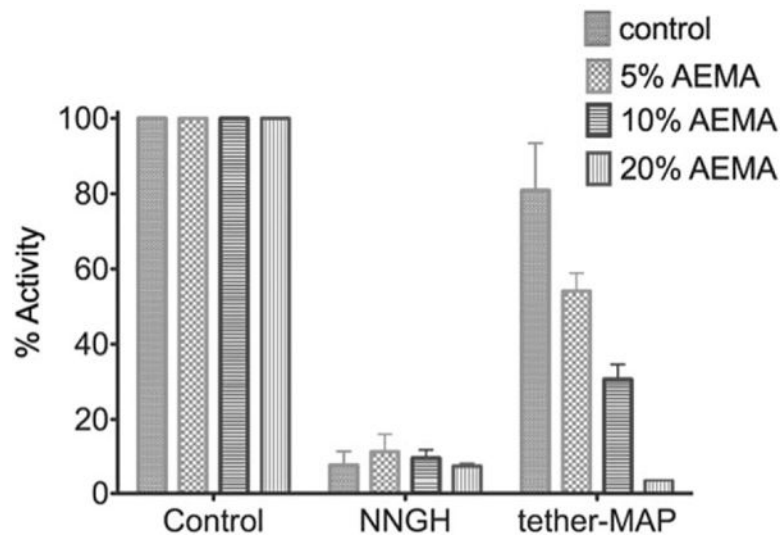


**FIGURE 6.** MMP-8 activity is inhibited by MAP-grafted polymer surfaces. Bar graph of MMP-8 fluorimetric RED assay carried out on control (0%), 5%, 10%, 15%, and 20% amine-containing polymers grafted with tether-MAP. The standard inhibitor NNGH was used as a control. [Color figure can be viewed in the online issue, which is available at [wileyonlinelibrary.com](http://wileyonlinelibrary.com).]